3-D Geological modelling: a siliciclastic reservoir case study from Campos Basin, Brazil

Ulisses Miguel Correia
Doutorando
Universidade Estadual de Campinas - UNICAMP
Departamento de Geologia e
Recursos Naturais do Instituto de Geociências
Campinas - São Paulo - Brasil
ulisses.correia21@gmail.com

Alessandro Batezelli
Professor Doutor
Universidade Estadual de Campinas - UNICAMP
Instituto de Geociências
Campinas - São Paulo - Brasil
abatezelli@ige.unicamp.br

Emilson Pereira Leite
Professor Doutor
Universidade Estadual de Campinas- UNICAMP
Instituto de Geociências
Campinas - São Paulo - Brasil
emilson@ige.unicamp.br

Abstract

Reservoir static modelling plays a fundamental role in the evaluation phase of a petroleum field. Integrated modelling allows a better understanding of how the local geology and depositional systems are related through the distribution of facies and petrophysical properties within the reservoir. In this study, geological static models of the siliciclastic Carapebus Formation of Campos Basin were built using subsurface data. The applied methodology was divided into five phases: (1) establishment of a conceptual model, (2) building of a structural model, (3) generation of 100 realizations of lithofacies using sequential indicator simulation, (4) generation of 100 realizations of porosity and permeability using sequential Gaussian simulation, and (5) validation of models by targeting both statistical and geological consistency. The obtained models are consistent and honor the conditioning data. A lithofacies constraint is crucial to better characterize the petrophysical properties distribution of the reservoir. A Dykstra-Parsons coefficient of V=0.52 characterizes this reservoir as moderately homogeneous.

Keywords: Campos Basin, Siliciclastic Reservoirs, Carapebus Formation, Static Modelling.

1. Introduction

The geological models, often called reservoir static models, play an essential role in the understanding of intrinsic spatial characteristics and features of the reservoirs. These models have been important to predict reservoir performance because they incorporate several information, such as static petrophysical properties within the stratigraphic layers and structural framework. Static models are also used to predict inter-well distributions of relevant properties, such as porosity and permeability. Furthermore, static reservoir models are improved through an iterative process in order to better quantify and assess uncertainty.

Cosentino (2001) and Deutsch (2002) point out that it is necessary to create consistent 3-D geological models.

Additionally, these authors suggest the application of geostatistical algorithms of sequential simulation, such as Gaussian and indicator to conduct the modelling process. Whereas sequential indicator simulation is suitable for categorical variables, the sequential Gaussian simulation is applied to continuous variables.

Ravenne (2002) and Remacre *et al.* (2008) emphasize that proportion curves are powerful tools for reservoir characterization, because they provide a better understanding on how the facies proportions vary within and between the wells with respect to a stratigraphic datum. Furthermore, these authors highlight that petrophysical properties should be constrained to facies proportions in order to get a better estimate of the petrophysical

distributions.

Dykstra and Parsons (1950) developed a criterion for quantifying reservoir heterogeneity based on the permeability distribution and the well-known coefficient of variation. Dykstra-Parsons coefficient takes values between 0 and 1 and, for most reservoirs this coefficient ranges between 0.5 and 0.9, from homogenous to heterogeneous.

Understanding the heterogeneities of the main reservoirs of the Campos Basin (Brazil), far from being a mature basin, has still been a challenge.

This study aims at building a 3-D geological model of the turbidite reservoir of the Carapebus Formation in the Campos Basin, in order to better understand and characterize reservoir heterogeneities.

2. Case study: Carapebus siliciclastic reservoir

2.1 Campos Basin setting

Campos Basin lies between the updip limits of the turbidites to the west, the Vitoria-Trindade Arch to the north, the Cabo Frio Arch to the south, and the boundary of the salt diapir region at water depths of ~2,200

m to the east. The basin is approximately 500 km long and 150 km wide encompassing nearly 120,000 km² of the Brazilian southeast offshore. It reaches up to 3,400 m of water depth.

Based on a compilation of previous works on Campos Basin, Winter *et al.* (2007) divide its stratigraphic evolution into five main chronostratigraphic megasequences, from early Cretaceous to Tertiary, as follows: (1) continental megasequence with three sin-rift phases where the first and the second are characterized by eolian and alluvial fan deposits, and the third is characterized by extensive strata of coquinas, calcarenites, calcilutites and shales; (2) evaporitic transitional megasequence with conglomerates and sandstones, followed by the formation of an evaporitic sea in the southern part of the basin; (3) shallow carbonate platform which developed most of the basin's shallow carbonates; (4) transgressive marine megasequence composed by calcilutites, marl and shales; this transgressive megasequence registered a gradual increase in depth recorded by the deposition of deep water turbidites; and (5) regressive marine megasequence where a modification in the sedimentation regime occurred, with the development of deltaic, fluvio-deltaic, terrigenous and carbonate platform depositional systems.

2.2 Carapebus reservoir description

According to Bruhn *et al.* (1998), the studied reservoir is part of the siliciclastic Carapebus Formation of Campos Group in Campos Basin. The age of the studied section of this reservoir ranges from Oligocene to Miocene. It was deposited by several turbiditic events in a regressive marine megasequence of deep water unconfined depositional systems (water depths between 1,000 to 2,000 m), defining unconfined sand lobes. In terms of grain size, medium to coarse sand are predominant. Porosity reaches 35% and permeability ranges roughly from 1,000 to 2,500 mD in the producing intervals, consisting of the most prolific turbidite reservoirs in the basin.

Bruhn (2001) measured porosity and permeability of core samples which allowed distinguishing two deposits in the Carapebus Formation reservoir both from Oligocene-Miocene. The author obtained porosity and permeability values of (1) 32% and 574 mD for thicker and poorly sorted deposits, and of (2) 26% and 2,434 mD for thinner and moderately well sorted deposits.

2.3 Data set

The data set was provided by the Brazilian National Agency of Petroleum, Natural Gas and Biofuels (ANP), and was comprised of four wells and eight 2-D seismic lines (Figure 1). All wells included gamma ray, density, sonic and resistivity logs, and descriptions of cores from two wells were available.
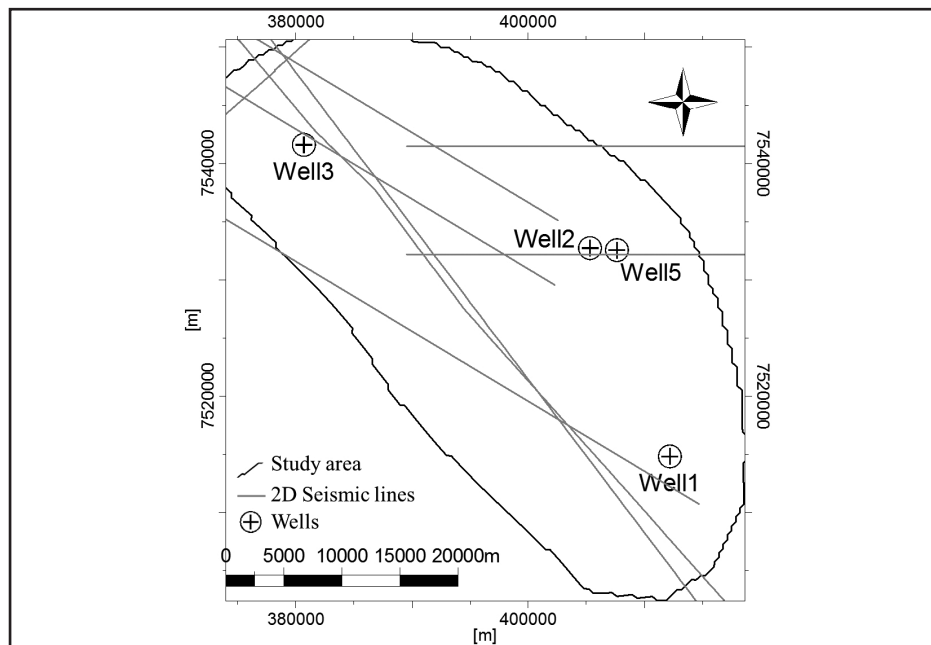

Figure 1
Data set location:
study area is limited by
the polygon (black), 2D seismic
lines (grey), and wells (black symbols).

3. Method

To conduct the 3-D geological modelling, the method proposed by Cosentino (2001) and Deutsch (2002) was applied using an academic license of Petrel 2013.1 software. It is a workflow where stratigraphy constrains the geostatistical grid geometry, which in turn supports the modelling (Figure 2). It comprises five phases:

Phase 1: Development and establishment of a consistent conceptual model emphasizing the depositional system, in order to identify the main expected scales and heterogeneities.

Phase 2: Structural modelling considering the stratigraphic layering, in order to get a suitable geostatistical grid which incorporates well-known heterogeneities, and has an adequate size estimated based on the computational power available. Well formation tops and interpreted seismic surfaces are used to define the vertical boundaries of the layers, while fault structures define lateral boundaries.

Phase 3: Cell-based lithofacies modelling within each previously es-

tablished stratigraphic layer, using the sequential indicator simulation algorithm. This should be performed for a number of realizations to ensure stability of the variance of the models. This geostatistical simulation uses vertical proportion curves taking into account facies distributions along stratigraphic layers (e.g. Ravenne, 2002; Remacre *et al.*, 2008).

Phase 4: Petrophysical modelling of porosity and permeability for each lithofacies realization, using the sequential Gaussian simulation algorithm. For the permeability modelling it might be necessary to develop a porosity-permeability transformation (Phi-K) from core data, in order to get a permeability log in uncored intervals. Therefore, this implies

that permeability will follow the porosity distribution.

Phase 5: Validation of the models based on statistical and geological consistency. This validation is carried out by analyzing the statistical parameters of the simulated and original distributions and by comparing overall results to those available in the literature.
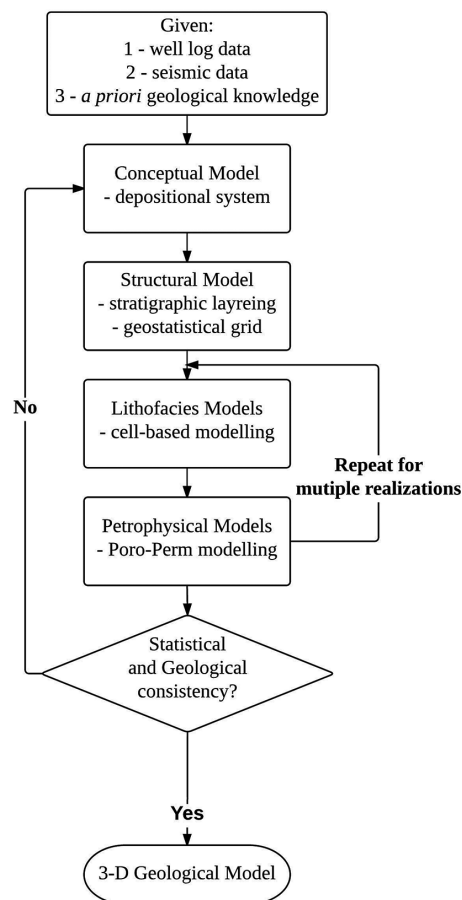

Figure 2
3-D geological modelling flow chart.

4. Application

The ideal conceptual model used to guide the modelling phase was the unconfined sand lobes defined by Bruhn *et al.* (1998).

Top and base reservoir surfaces were interpreted from the available seismic data, based on concepts of seismic stratigraphy and geomorphology (see e.g. Posamentier & Kolla, 2003).

Time-to-depth conversion was made using a simple layer cake velocity model built with well checkshots.

To establish lithofacies, a logic function was applied to gamma ray logs, distinguishing three main lithofacies: shale, sandstone and marl. These were derived from core samples which 12 well lithotypes were identified and then resampled

to three representative lithofacies.

The log-derived porosity was calculated from the bulk density log based on Asquith & Gibson (1982) equation. For this calculation, it was considered that the siliciclastic rocks do not have significant shale content in their composition (lower than 15% within reservoir intervals). The used equation is defined as follows:

$$\text{total porosity} = \frac{\text{matrix density - density log}}{\text{matrix density - fluid density}}$$

where, for this study, matrix density = 2.644 g/cm³ and fluid density = 1.025 g/cm³.

The log-derived permeability curve was fitted using core data and it reads as follows:

$$\log permeability\,(mD) = 4.09121\,(porosity) - 1.30056$$

where, for this study, a correlation coefficient of r = 0.82 was obtained.

The constructed geostatistical grid is a corner point with 2.5 million cells, defined by 400 x 400 m in the horizontal directions and 1.5 m in the vertical direction, with 123x121 cells and 170 cell layers.

It was required to upscale the modelled properties to the grid resolution using averaging methods: (1) for lithofacies, the "most of" was applied, (2) for the log-derived porosity, the arithmetic mean was applied, and (3) for the log-derived permeability, the geometric mean was applied (see e.g. Durlofsky, 2005).

A structural analysis was carried out with the aid of experimental variograms. These variograms were computed along two horizontal directions, NW and NE and the vertical direction, as they are well-known as major Campos Basin's turbidite deposition (Figure 3). It is possible to verify the degree of uncertainty

in variograms owed to the lack of data. The spherical model was adopted for both lithofacies and petrophysical modelling, even if the proximity of data points to the origin was not linear. It was possible to infer that for the vertical direction, both properties are characterized by a high variability, and the data points of experimental variograms are distantly spaced. Table 1 shows the variogram parameters for the fitted models of lithofacies and petrophysical properties.
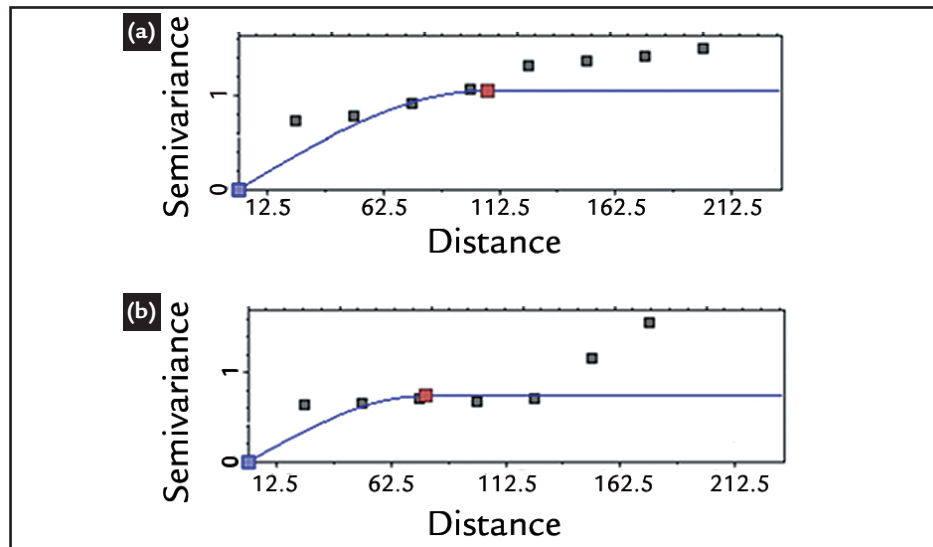

Figure 3
Experimental (dots) and modelled (curve) vertical variograms: a - lithofacies; b - petrophysics.

Property	Range			Sill	Nugget
	NW	NE	Vertical		
Lithofacies	20000	10000	100	1.0	0
Petrophysical	20000	15000	100	0.5	0

Table 1
Variogram model parameters for lithofacies and petrophysical properties.

For the lithofacies modelling, 100 realizations of the sequential indicator simulation algorithm were performed. For the petrophysical models, 100 realizations of the sequential Gaussian simulation were performed, conditioned by the lithofacies models. Permeability was co-simulated with porosity as a secondary property by applying collocated co-kriging. A locally varying correlation coefficient from porosity was used, assigning one value for each grid cell.

The global vertical proportion curve includes high percentages of marl, but low percentages of sandstone and shale. Emphasis can be given to the top and central layers (10 to 50 and 80 to 120), defined by 50% to 70% of sandstone facies. These heterogeneities were characterized by a total of 170 stratigraphic layers with thickness of 1.5 m each, in order to capture the vertical variation of the well logs (Figure 4).

According to Bruhn *et al*. (1998) and Machado *et al*. (2004), lobes deposited over several time events are a common feature of this reservoir in proximal areas.

The heterogeneity of this reservoir was quantified by calculating the Dykstra-Parsons coefficient of permeability variation, as follows:

$$V = \frac{Log\,(K)_{50} - Log\,(K)_{84.1}}{Log\,(K)_{50}}$$

where $Log(K)_{50}$ - permeability mean; $Log(K)_{84.1}$ - mean plus one standard deviation.
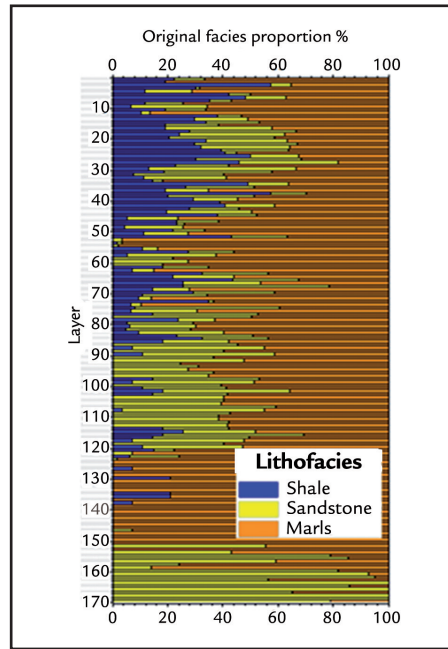
Figure 4
Global vertical
proportion curve of lithofacies.

5. Results and discussion

One example of equiprobable realization of the obtained lithofacies and petrophysical models is shown in Figures 5 to 7.
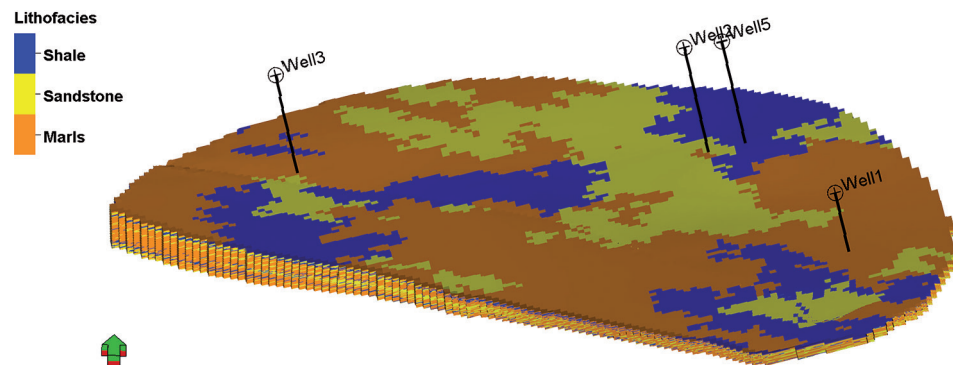

Figure 5
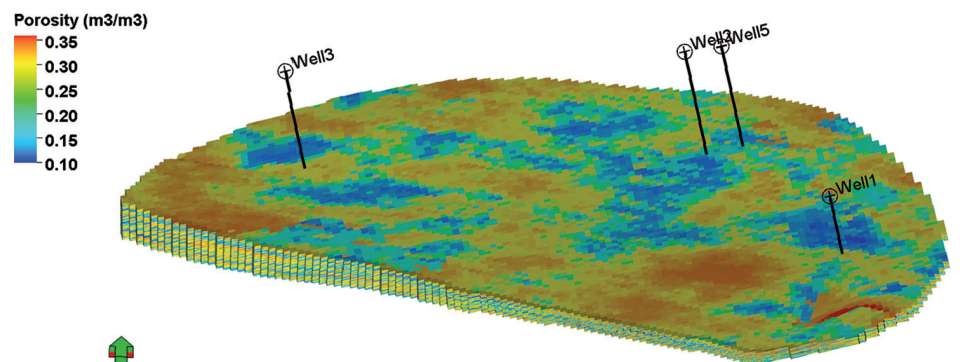Lithofacies model realization #37.

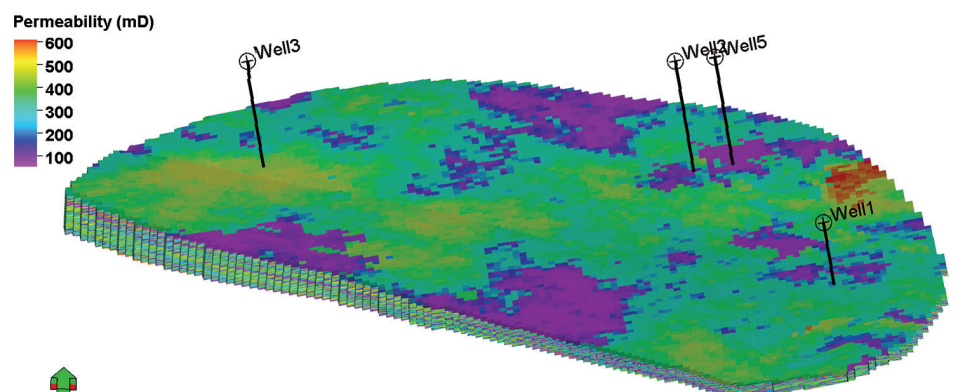Figure 6
Porosity model realization #37.

Figure 7
Permeability model realization #37.

The facies proportions obtained in the lithofacies models were in accordance with the global vertical proportion curve. The simulated proportion for the shale was 14%, for the sandstone was 26% and for the marl was 60% (Table 2).

The value of log-derived porosity averages 25% and ranges from 0% to 40%. The simulated value averages 25% and ranges from 10% to 36% (Table 3).

Core-measured permeability ranges from 107 to 864 mD, the simulated log ranges from 51 to 610 mD and the geometric mean is 271 mD (Table 4).

Both porosity and permeability are characterized by a bi-modal distribution. These bi-modal distributions helped to distinguish between reservoir and non-reservoir potential facies. By having bi-modal distributions, careful analysis of the descriptive statistics is required.

Lithofacies models	Original proportion (%)	Simulated proportion (%)	Delta (%)
Shale	15.3	13.9	-9.2
Sandstone	25.9	26.1	0.8
Marl	58.8	60.0	2.0

Table 2
Original lithofacies, simulated proportions and difference (delta) between proportions over 100 realizations.

Porosity (%)	Min	Max	Mean	Standard deviation	Delta mean (%)
3-D models	9.9	36.3	24.7	7.3	
well logs	0.0	40.0	25.0	8.0	-1.2

Table 3
Descriptive statistics of porosity from the well log data and from the 3-D model over 100 realizations.

Permeability (mD)	Min	Max	Mean	Standard deviation	Delta mean (%)
3-D models	51	610	271	138	
well logs	20	898	267	148	1.5

Table 4
Descriptive statistics of permeability from the well log data and from the 3-D model over 100 realizations.

Differences between original and simulated distributions are presented in Figures 8 and 9. These differences are caused by the employed upscaling procedure and by the spatial density of the data.

For the proportions of the lithofacies models, there were differences of -9.2% for shale, +0.8% for sandstone, and +2.0% for marl. For the mean of the porosity models, there was a difference of -1.2%. For the mean of the permeability models, there was a difference of +1.5%.

It is possible to assess the bi-modal distributions of the petrophysical parameters by considering different sources of the turbidite depositional system, which comprises at least five different main features. According to Bruhn (2001) those features are: (1) complex external geometry, (2) fine-muddy interbedded deposits, (3) discontinuous calcitic concretions, (4) cemented sandstones and conglomerates, and (5) porosity and permeability variation with deposits grain size and sort.
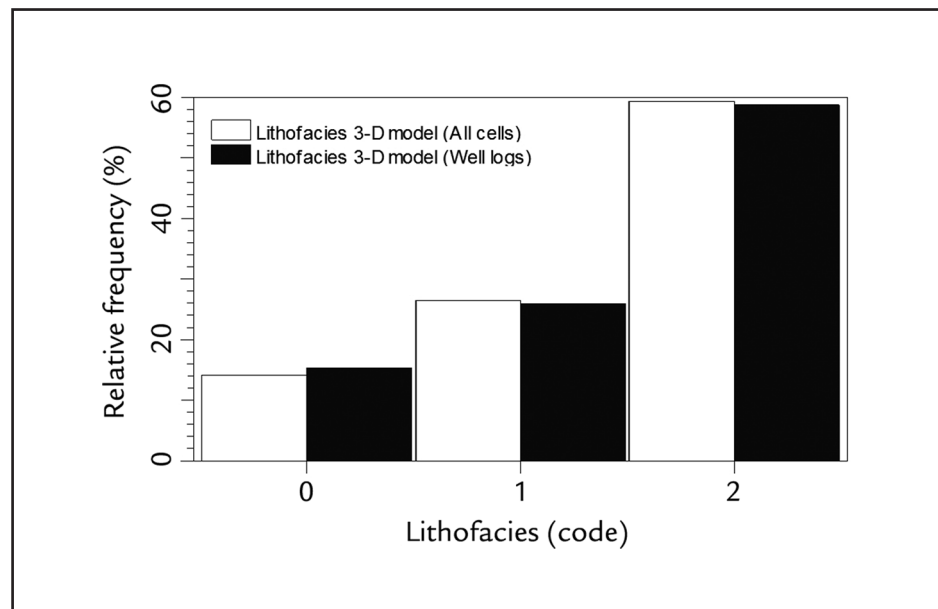

Figure 8
Histogram reproduction on lithofacies realization #37.
0 - shale, 1 - sandstone, 2 - marl.
Black bars: original histogram.
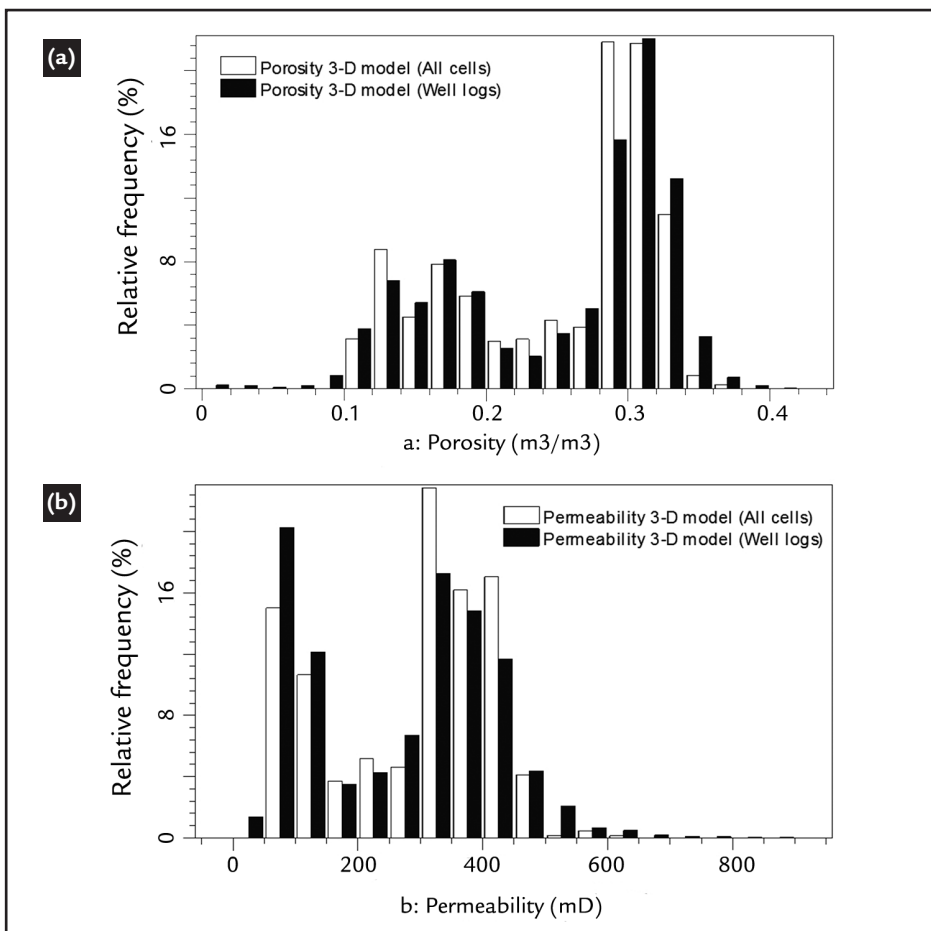White bars: simulated histogram.

Figure 9
Histogram reproduction
on realization #37. a - porosity;
b - permeability. Black bars: original
histogram. White bars: simulated histogram.

It was possible to compare the porosity and permeability results with those achieved by Bruhn (2001) in core samples of Oligocene-Miocene. Comparing these results with the thicker deposits presented in Bruhn (2001), the porosity obtained in this study is 22% lower and the permeability is 6% higher. Comparing with the thinner deposits, the porosity obtained is 5% lower and the permeability is 74% lower.

Dykstra-Parsons coefficient of permeability variation for sandstone lithofacies of the studied reservoir is V=0.52. This coefficient points to a moderately homogeneous reservoir. The obtained coefficient is equal to that calculated by Dutton *et al.* (2003) for a deep water siliciclastic case study from Ramsey reservoir in the East Ford field. Moreover, this coefficient

is within the range of most reservoirs.

The results of several studies show that these turbidite deposits have different types and can be fairly complex. In addition, these reservoirs are distinguished based on their grain size, net-to-gross ratio, external geometry, processes and depositional settings (Bruhn *et al.*, 2003; Machado *et al.*, 2004).

This study has two main limitations: (1) the low data density and the data distribution, which affected directly the variogram modelling, and (2) Phi-K transformation, knowing that the permeability does not follow the porosity distribution.

As pointed by Chambers et al. (2000), in a situation with lacking data, the parameters chosen in the sequential indicator simulation and sequential Gaussian simulation algorithms certainly impact

the results.

Despite these limitations, the histograms of the simulated values reproduce those of the original values within an acceptable error level. Therefore, by applying the Cosentino (2001) and Deutsch (2002) methodology for integrated reservoir studies it was possible to infer the relationships between geology and depositional systems of this reservoir.

The observed differences between simulated and original distributions might be straightforwardly assigned to the sparse data set used to perform the geological modelling in this study. Additionally, these differences may also be assigned to the change-of-support effect, produced by distinct size support of data set and model grid; and the smoothing character of the kriging algorithm.

6. Conclusions

The main conclusions of this study are:
1. The obtained models reveal geological and statistical consistency, with tolerable statistical variations.
2. The geostatistical model grid plays a major role in defining the vertical layering of the global vertical proportion curve.
3. Lithofacies models show minor

differences between original and simulated proportions (lower than 10%).
4. Petrophysical models conditioned to lithofacies presents very low differences with respect to the original distributions (1.2% for porosity and approximately 1.5% for permeability).
5. Lithofacies constraints are essen-

tial to an improved characterization of the distribution of petrophysical properties in the reservoir.
6. Phi-K transformation outlines the permeability models statistical outputs because it assumes a linear correlation with the porosity distribution.

Generating lithofacies models is

essential for properly characterizing the reservoir, due to its relationship with the petrophysical properties distribution. Geological consistency needs to be assessed and validated over an iterative process of producing and fitting models, considering that these are digital representations of a highly complex physical reality.

For further work it is recommended to assess different geologic scenarios by varying the variogram parameters. It will help to conduct sensitivity analysis and uncertainty quantification in volumetric estimation.

7. Acknowledgements

8. References

ASQUITH, G. B., GIBSON, C. R. *Basic well log Analysis for geologists.* Oklahoma, Tulsa: AAPG, 1982. 216p.

BRUHN, C. H. L. Contrasting types of Oligocene / Miocene Giant Turbidite Reservoirs from deep water Campos Basin, Brazil. In: *AAPG Distinguished Lecture*, 2001.

BRUHN, C. H. L., BARROSO, A. S., LOPES, M. R. F., SARZENSKI, D. J., ABREU, C. J., SILVA, C. M. A. High-resolution stratigraphy and reservoir heterogeneities of upper Albian Turbidite Reservoirs of Albacora Field, Campos Basin, Offshore Brazil. In: AAPG ANNUAL CONVENTION. Salt Lake City, Utah: AAPG, 1998.

BRUHN, C. H. L., GOMES, J. A. T., LUCCHESE JR, C. D., JOHANN, P. R. Campos basin: reservoir characterization and management – historical overview and future challenges. OTC 15220. In: OFFSHORE TECHNOLOGY CONFERENCE, Society of Petroleum Engineers, Houston, Texas, USA. 2003.

CHAMBERS, R. L., YARUS, J. M., HIRD, K. B. Petroleum geostatistics for nongeostatisticians – Part 2. *The Leading Edge*, v. 19, n. 6, p. 592-599, 2000.

COSENTINO, L. *Integrated reservoir studies.* Paris: Editions Technip, 2001. 310p.

DEUTSCH, C. V. Geostatistical reservoir modeling. In: *Applied Geostatistics Series.* New York: Oxford University Press, Inc, 2002. 376pp.

DURLOFSKY, L. J. Upscaling and gridding of fine scale geological models for flow simulation. In: 8TH INTERNATIONAL FORUM ON RESERVOIR SIMULATION. Stresa, Italy: Iles Borromees, June 20-24, 2005.

DUTTON, S. P., FLANDERS, W. A., BARTON, M. D. Reservoir characterization of a Permian deep-water sandstone, East Ford field, Delaware basin, Texas. *AAPG Bulletin,* v. 87, n. 4. p. 609-627. 2003.

DYKSTRA, H., PARSONS, H. L. The prediction of oil recovery by waterflooding. In: *Secondary Recovery of Oil in the United States.* (2nd Ed.). New York: API, 1950. p. 160-174.

MACHADO, L. C. R., KOWSMANN, R. O., ALMEIDA JR., W., MURAKAMI, C. Y., SCHREINER, S., MILLER, D. J., ORLANDO, P., PIAUILINO, V. Geometria da porção proximal do sistema turbidíticos moderno da Formação Carapebus, bacia de Campos; modelo para heterogeneidades de reservatório. *Boletim de Geociências da Petrobras,* v. 12, n. 2, p. 287 – 315, maio./nov. 2004.

POSAMENTIER, H. W., KOLLA, V. Seismic geomorphology and stratigraphy of depositional elements in deep-water settings. *SEPM Journal of Sedimentary Research,* v. 73, n. 3, p. 367–388, 2003. doi: 10.1306/111302730367

RAVENNE, C. Stratigraphy and oil: a review. Part 2 - characterization of reservoir and sequence stratigraphy: quantification and modeling. Oil & Gas Science and Technology – *Rev. IFP,* v. 57, n. 4, p. 311-340, 2002. doi: 10.2516/ogst:2002021

REMACRE, A. Z., NORMANDO, M. N., SANCEVERO, S. S. Krigagem das proporções utilizando a krigagem da média: uma ferramenta auxiliar na modelagem de reservatórios. *Revista Brasileira de Geociências,* v. 38, n. 1 – suplemento, p. 82-77, 2008.

WINTER, W. R., JAHNERT. R. J., FRANÇA, A. B. Bacia de Campos. *Boletim de Geociências da Petrobras,* v. 15, n. 2, p. 511-529, maio/nov. 2007.